



---

# SPRAY DRAG OF SURFACE-PIERCING STRUTS

by  
Richard B. Chapman  
Sensor And Fire Control Department

September 1971

---



Approved for public release; distribution unlimited.

---



NAVAL UNDERSEA RESEARCH AND DEVELOPMENT CENTER, SAN DIEGO, CA. 92122

AN ACTIVITY OF THE NAVAL MATERIAL COMMAND

CHARLES B. BISHOP, Capt., USN  
Commander

Wm. B. McLEAN, Ph.D.  
Technical Director

The work reported was done from September to November 1970, and was sponsored by the NUC Independent Exploratory and Development Funds as part of the "New Vehicle and Sonar Studies."

Released by  
T. G. LANG, Head  
Advanced Concepts Group

Under authority of  
W. D. SQUIRE, Head  
Sensor and Fire  
Control Department

ii

## SPRAY DRAG OF SURFACE-PIERCING STRUTS

R. B. Chapman, Mechanical Engineer  
Naval Undersea Research and Development Center  
San Diego, California 92123

### Abstract

Spray drags were measured with a series of nine surface-piercing struts operated in fourteen configurations at Froude numbers between 5 and 6. Empirical equations were deduced and compared with earlier data. The strut surface-area wetted above the static waterline by the spray sheet was determined from photographs and used to show that the frictional drag of the spray sheet flowing over the strut was the primary source of the measured spray drag. The mass flow rate contained in the spray sheet was measured indirectly. Following these experiments horizontal rails were attached to three struts and produced significant reductions in the spray drag of each. In later experiments the spray drag at smaller Froude numbers was determined by subtracting theoretical frictional and wave-making drag from drag measured on low aspect ratio struts.

### List of Symbols

c	chord length
t	strut thickness
x	distance from leading edge to point of maximum thickness (forebody length)
q	dynamic pressure, $\frac{1}{2}\rho V^2$
$\rho$	density of water, 1.94 slugs/ft <sup>3</sup>
V	free stream velocity
D <sub>total</sub>	total drag on the strut
D <sub>spray</sub>	spray drag
D <sub>tip</sub>	tip drag
D <sub>v</sub>	drag caused by the upward acceleration of the spray
X	section drag/depth of submersion
d	depth of strut tip below the waterline
A	area of strut in the plane of the undisturbed free surface, waterplane area
C <sub>0</sub>	spray drag coefficient, $D_{\text{spray}}/qct$
C <sub>1</sub>	spray drag coefficient, $D_{\text{spray}}/qA$
T	thrust of spray striking plate
V	mean velocity of spray striking plate
M	mass rate of flow of spray
C <sub>M</sub>	mass flow rate coefficient, $M/\rho Vt^2$
F	Froude number, $V/\sqrt{gc}$
g	acceleration of gravity, 32.2 ft/sec <sup>2</sup>
h	mean maximum height of spray

### Introduction

Work was done to determine the amount of spray drag acting on a surface-piercing strut suitable for use on a semi-submerged ship. Means of reducing this drag were also investigated. (A semisubmerged ship concept has been developed. (1) The ship consists of a pair of totally submerged hulls connected to a platform held above the waterline by two pairs of surface-piercing struts.) Wave drag reaches a maximum when the Froude number based on chord length is approximately 0.5. (2) Wave formation and wave drag drops off rapidly at higher Froude

numbers and is replaced by a thin film of water which flows over the strut above the waterline leaving a spray sheet behind the trailing edge. Data indicates (2,3) that wave drag is negligible and spray drag is independent of Froude number for Froude numbers of about three or greater.

Two empirical formulations for spray drag are those of Hoerner (2) and Savitsky & Breslin (3) Hoerner combined his own results with data from Coffee and McKann, (4) Kaplan, (5) and others to deduce the empirical relationship

$$D_{\text{spray}} = 0.24qt^2 \quad (1)$$

for thickness to forebody ratios (t/x) less than about 0.4, and

$$D_{\text{spray}} = 0.12qt^2 \quad (2)$$

for blunter bodies. Savitsky and Breslin (3) measured the spray drags for a series of airfoils with t/c = 10, 20, and 30% and x/c = 30%. From their data they deduced

$$D_{\text{spray}} = 0.03 qct + 0.08qt^2 \quad (3)$$

Equation 3 results from fitting a straight line for  $D_{\text{spray}}/qct$  over a limited range of t/c and does not contain the discontinuity apparent in Eqs. 1 and 2. The spray drags measured by Savitsky and Breslin are clearly greater than those predicted by Hoerner, perhaps because they used relatively blunt airfoils. This difference suggested that strut form may be an important factor in spray drag.

Although the spray drag estimate of Hoerner is significantly less than that of Savitsky and Breslin, both estimates indicate that spray drag could make a major contribution to the residual drag of a high-speed semisubmerged ship. However, several factors may lower the spray drag of such ships.

1. Spray drag may depend on strut form. Selection of a favorable shape could minimize spray drag.

2. If spray drag is caused primarily by the friction of the spray sheet, the drag on a full scale strut would be considerably less than on a model due to the reduced coefficient of friction at high Reynolds numbers. This effect cannot be investigated directly with models, but any evidence that spray drag is caused by friction of the spray sheet acting on the strut would tend to support this hypothesis.

3. Appendages may be added to the struts which would cause the spray to separate and possibly reduce drag.

4. Maximum speeds of semisubmerged ships correspond to Froude numbers of about two or less. Some wave drag will still be present at these speeds and the spray sheet may not be fully developed. Spray drag is more difficult to characterize at these

10-11 2021

Froude numbers since wave drag must be accounted for and the results will depend on Froude number. Equations 1 through 3 are based on experiments made at high Froude numbers.

To gain further insight into the problem of spray drag, two series of exploratory experiments were conducted. The first set was made at high Froude numbers with a number of struts of a variety of shapes. The influence of strut shape, comparison with previous results, and an understanding of the mechanism of spray drag were emphasized in this series of tests. A second series of tests was made with larger struts at lower Froude numbers that corresponded to the high-speed range of semisubmerged ships. These tests were recently conducted at the Lockheed Towing Basin in San Diego. The main body of this report will concern the first series of tests. Some results from the second series are given in Appendix A.

#### Description of the Strut Models

Nine strut models were fabricated from wood. Five of these were also tested with the direction of flow reversed, making a total of fourteen configurations. The first eight models had no angle of rake and six-inch chords. The ninth was raked 45° and had a chord length of  $6\sqrt{2} \approx 8.5$  inches. The first eight struts all had t/c ratios of 12, 16, or 21%. For each of these three ratios, two struts of the double arc type composed of two pairs of circular arcs were built, a symmetric strut with x/c = 50%, and an asymmetric strut with x/c = 35% or 65% depending on the direction of flow. The other three struts were a 16%-thick strut with a cusp on one edge and a wedge on the other, a 16%-thick 66-series airfoil, and a 16%-thick symmetric double-arc strut raked 45° to produce an effective t/c of about 11.3%. All struts had rounded tips and 0.25-inch wide sandstrips starting 0.75 inches from both leading and trailing edges. The nonraked struts were all 22-inches long. The strut forms are listed in Table 1.

#### Measurement of Spray Drag

The strut models were tested with freestream velocities of 20, 22, and 24 ft/sec. Based on a 6-inch chord these velocities correspond to Froude numbers between 5.0 and 6.0 and Reynolds numbers of about  $10^6$ . These Froude numbers are sufficiently high to assure that the test data is not strongly effected by Froude number. The measured values of section drag on the models indicate that the flow was turbulent.

Each configuration was tested at fifteen or more depths of submergence from a minimum of 3.4 inches. The drag on each strut was found to be a linear function of the submerged depth. The slope was identified with the two-dimensional section drag and the intercept was identified with the sum of the changes in drag due to the strut tip and the free surface. In equation form the relationship is

$$D_{total} = Xd + D_{spray} + D_{tip}, \quad (4)$$

where X is the section drag in lbs/ft. The tip drag was estimated with an empirical equation for rounded tips<sup>(2)</sup>

$$D_{tip} \sim -0.02qt^2. \quad (5)$$

The negative tip drag is apparently due to the three-dimensional nature of the flow near the tip. This tip drag correction is roughly of the same magnitude as the scatter in the spray drag data.

#### Spray Drag Results

Results of calculations from Eqs. 4 and 5 are listed in Table 1. Two spray drag coefficients are presented:  $C_D$  based on the area  $ct$ , and  $C_{D1}$  based on the waterplane area  $A$ , an important parameter for the semisubmerged ship. The coefficient  $C_D$  is plotted against t/c in Figure 1 for struts of the double arc form. Also shown are empirical equations and data.<sup>(2,3)</sup> A dependence of spray drag on strut form is evident in the present data. Struts with x/c = 35% produced the most spray drag and struts with x/c = 65% produced the least.

Lines similar to Eq. 3 were fitted for each of the three groups of double arc struts which resulted in the following empirical equations:

$$C_D = 0.003 + 0.06 t/c \quad \text{when } x/c = 65\%, \quad (6)$$

$$C_D = 0.011 + 0.08 t/c \quad \text{when } x/c = 50\%, \quad (7)$$

and

$$C_D = 0.009 + 0.013 t/c \quad \text{when } x/c = 35\%. \quad (8)$$

These equations are quite rough because of data scatter and the uncertainty of the tip drag estimate.

Both the cusp and the wedge leading edges of strut 2 produce less drag than strut 1. After the waterplane area is taken into account, however, this advantage becomes negligible. The double-arc strut swept 45° appears to offer a savings in spray drag contrary to other conclusions<sup>(4)</sup> based on airfoils swept 30°, that the spray drag of a swept strut depends only on its waterplane form.

#### Comparison With Previous Results

The empirical formula of Hoerner is partially based on the spray drags of a 13%-thick symmetric double arc tested by Benson and Land and a 15%-thick asymmetric double arc with x/c = 40% tested by Kaplan.<sup>(5)</sup> The 13% and 15%-thick double-arc struts produced  $C_D$  coefficients of 0.026 and 0.028, respectively. These values are very close to those predicted by Eq. 9 and within 20% of those predicted by Eq. 8. Kaplan found that the 15%-thick double arc was not sufficiently asymmetric to cause a detectable change in the spray or section drag when the direction of flow was reversed. Hoerner also uses measurements apparently made with 15% and 30%-thick struts with x/c = 40%. The shapes of these struts were not indicated, but they were probably lenticular. The spray drags of these struts were also independent of the direction of flow. The corresponding value of  $C_D$  for both thicknesses was 0.036. This is about 50% greater than predicted by Eq. 7 for the 15%-thick strut but very close to the predicted value for the 30%-thick strut. In general, spray drags used by Hoerner are larger than predicted by Eq. 7 but are not inconsistent when differences and experimental error is taken into account.

Figure 2 shows the spray drags reported by Coffee and McKann<sup>(4)</sup> for 12%- and 21%-thick 66-series airfoils together with the spray drag measured in the present experiment with 16%-thick airfoil of the same series. The much lower spray drag of the reversed airfoil 8B again illustrates the influence of strut form. In interpreting this result, the uncertainty introduced by tip drag and the fact that the struts used by Coffee and McKann had square tips should be considered. A straight line fitted through the points in Figure 2 gives the approximate formula

**Table I. Spray Drag and Spray Drag Coefficients for Various Strut Configurations**

Strut Configuration	Speed, ft/sec	t/c	x/c	Type*	Spray Drag, lb	C <sub>0</sub>	C <sub>1</sub>
1	24	<b>0.16</b>	<b>0.50</b>	D.A.	<b>0.515</b>	0.023	0.035
	22				0.43	0.022	0.033
	20				0.40	0.024	0.036
<b>2A</b>	24	0.16	0.50	<b>CSP</b>	0.37	0.017	0.030
<b>2A</b>	22				0.34	0.018	0.032
<b>2A</b>	20				0.305	0.018	0.033
<b>2A</b>	20				0.30	0.018	0.032
<b>2B</b>	24	0.16	0.50	WDG	<b>0.375</b>	0.017	0.030
<b>2B</b>	22				0.355	0.018	0.033
<b>2B</b>	22				0.335	0.017	0.031
<b>2B</b>	20				0.28	0.017	0.030
<b>3A</b>	24	0.16	0.35	D.A.	0.71	0.032	0.048
<b>3A</b>	22				0.585	0.031	0.046
<b>3A</b>	20				0.48	0.030	0.044
<b>3B</b>	24	0.16	0.65	D.A.	0.225	0.010	0.015
<b>3B</b>	22				0.21	0.011	0.016
<b>3B</b>	20				0.225	0.013	0.020
4	24	0.12	0.50	D.A.	0.37	0.022	0.033
4	22				0.315	0.022	0.033
4	20				0.255	0.021	0.031
5A	24	0.12	0.35	D.A.	0.385	0.023	0.034
<b>5A</b>	22				0.365	0.026	0.038
<b>5A</b>	20				0.285	0.024	0.036
5B	24	0.12	0.65	D.A.	0.16	0.010	0.014
<b>5B</b>	22				0.165	0.012	0.017
<b>5B</b>	20				0.12	0.010	0.015
6	24	0.21	0.50	D.A.	0.87	0.030	0.044
6	22				0.695	0.028	0.042
6	20				0.59	0.029	0.043
7A	24	0.21	0.35	D.A.	1.05	0.036	0.053
7A	22				0.855	0.035	0.052
7A	20				0.795	0.039	0.058
7B	24	0.21	0.65	D.A.	0.475	0.016	0.024
<b>7B</b>	22				0.400	0.016	0.024
7B	20				0.345	0.017	0.025
<b>8A</b>	24	0.16	0.50	FOIL	0.70	0.031	0.046
<b>8A</b>	22				0.60	0.032	0.047
<b>8A</b>	20				0.50	0.032	0.048
<b>8B</b>	24	0.16	0.50	<b>REV</b>	0.28	0.013	0.019
<b>8B</b>	22				0.23	0.012	0.018
8B	20				0.26	0.017	0.025
9	24	0.16	0.50	<b>SWP</b>	0.485	0.015	0.023
9	22				0.43	0.016	0.022
9	20				0.36	0.016	0.023

\*D.A. = Double Arc; CSP = Cusped Leading Edge; WDG = Wedge Leading Edge; FOIL = 66-Series Foil; REV = Reversed Foil; SWP = Swept Strut

$$C_0 = 0.036 - 0.03 t/c. \quad (9)$$

Note that the spray drag of the airfoil is similar to that of the asymmetric double arc strut of the same thickness in either orientation. This indicates that spray drag is not simply a function of x/c but depends on the overall shape.

#### Appearance of the Spray Sheet

The spray sheets appeared quite different for the various strut configurations. Photographs were made of ten representative configurations. The spray sheets produced at 10 and 24 ft/sec are shown in Figures 3 through 12. As these photographs show, spray is a somewhat misleading term for the smooth, continuous sheet which breaks up only after leaving the trailing edge. Separation

of the sheet from the strut was never observed. The sheet is thickest near the free surface and grows thinner further up the strut until it is terminated by a thick lip of slowly moving liquid believed to result from momentum loss caused by skin-friction. Near the top the sheet is very thin and the liquid may lose most of its horizontal velocity and move downward under the influence of gravity to collect in a lip. This should be most evident at low Froude numbers. The lip is, in fact, more obvious at lower speeds.

Note the differences in the spray sheets formed by the various struts. The sheet formed by the airfoil, shown in Figure 11, climbs the leading edge to over half a chord above the waterline. Similar behavior is displayed by sheets formed on airfoils.<sup>(4)</sup> In contrast, sheets formed on double arc struts leave the waterline at various angles. Steeper angles are associated with greater spray

drags. Another variation is the **cusped** strut configuration 2A which forms its sheet a small distance behind the leading edge.

### Spray Drag as a Function of Wetted Surface Area

It is evident that strut configurations which produce large spray sheets also have large spray drags. This observation is made quantitatively in Figure 13 which plots the spray drag of the photographed configurations at 24 ft/sec against the strut surface area wetted by the spray. Also plotted is the theoretical drag for turbulent flow at 24 ft/sec over a flat plate with a six-inch chord and surface area equal to the area wetted by the spray. There are a number of mechanisms which could cause the spray drag to depart from this value.

1. The horizontal component of the sheet velocity may not equal the free stream velocity.
2. Flow of the spray sheet may not be fully turbulent.
3. Another drag mechanism is the kinetic energy associated with the upward motion of the spray sheet.
4. Although there is no evidence of spray sheet separation, the spray sheet may contribute some pressure drag above the waterline.
5. At small distances below the waterline the flow will not be purely two-dimensional. The spray may have a favorable effect of relieving pressure drag near the free surface. This effect may contribute to the low values of spray drag measures on struts with  $x/c = 65\%$ .

Despite all these possible mechanism, the total area wetted by the spray sheet appears to be the controlling factor in the spray drag of all photographed struts with the possible exceptions of configurations 3B and 5B. Note that the small spray drag coefficient of the swept strut, 9, can be explained by the small wetted surface area.

Figure 13 includes data<sup>(4)</sup> for the 12% and 2 1/4% thick airfoils at 5 1 ft/sec. Since these foils had no turbulence stimulators, their section drag coefficients indicate that the skin-friction was less than in the fully turbulent case. To compensate for this reduced skin-friction, the spray drags of these points in Figure 13 have been multiplied by the ratio of the section drag coefficient of strut 5A to that of the 12% thick airfoil.<sup>(4)</sup> These compensated drags appear in Figure 13 only.

### Flow Rate of the Spray Sheet

Measurement of the properties of the spray sheet affords insight into the problem of spray drag. A simple experiment of this type was made by measuring the thrust caused by the spray striking a large flat plate mounted about one foot behind the trailing edge of a strut. The bottom of the plate was held approximately a quarter of an inch above the waterline. Measurements for each strut model were made at velocities of 20 and 24 ft/sec. In all cases the plate was ahead of the point where the spray would attain its maximum height in the absence of the plate. Of course a portion of the sheet leaving the trailing edge at a low angle and close to the waterline might fall back into the stream before striking the plate, but this portion is of little interest.

Table 2 lists the thrust T on the plate caused by spray sheets formed by each strut configuration. This thrust should equal the momentum flux of the spray striking the plate. Comparison with spray drags measured on the same struts indicate that friction can make a significant reduction in the momentum of the spray sheet, particularly for the thinner struts, but enough momentum is left to create a large pressure drag on any object the spray may strike. Also listed is the mass rate of flow M calculated with the approximation that spray drag is entirely due to the spray sheet being slowed below the free stream velocity V. Then, the mean velocity of the spray that leaves the strut is

$$V' = TV / (T + D_{\text{spray}}) \quad (10)$$

and the mass rate of flow is

$$M = (T + D_{\text{spray}}) / V. \quad (11)$$

The mass flow appeared to be concentrated in the lower portion of the spray sheet. The mass rate of flow of roughly the upper three-quarters of the sheet formed at 24 ft/sec by strut 2B was measured when the stream was captured in a bucket. About 1.5 lbs/sec entered the bucket, which indicates that the lower quarter of the sheet contained about half of the mass flow.

The mass rate of flow is nearly independent of strut form despite the wide range of forebody lengths. A coefficient based on strut thickness,

$$C_M = M / \rho V t^2, \quad (12)$$

is presented in Table 2. This coefficient should be a function of  $t/c$  and the Froude number. As shown in Figure 14, the data is well represented by

$$C_M = 3.7 Ft/c = 3.7 Vt/c \sqrt{gc}. \quad (13)$$

It should be emphasized that this empirical equation is based on a very limited range of data. It is reasonable, however, to expect  $C_M$  to increase with Froude number. Then skin friction will have a proportionally greater influence on the flow of the spray sheet at lower Froude numbers.

It is possible to estimate the drag caused by the energy dissipated to produce the upward acceleration of the spray. If M is the mass rate of flow and h is the mean maximum height attained by the fluid elements of the spray, this contribution to the drag is

$$D_v = Mh / V'. \quad (14)$$

In all cases this drag is a small fraction of the measured spray drag. For example,  $M = 3.4$  lbs/sec and  $V' = 20$  ft/sec for strut I at 24 ft/sec. A generous estimate for h of five inches results in a drag of about 0.07 lbs.

### Reduction of Spray Drag

Strut drag, a combination of spray drag and section drag, may be minimized by a proper choice of the strut form. Struts as thick as 2 1/4% can be eliminated, but for fixed waterplane area and depth of submergence, the symmetric double-arc struts with  $t/c = 12\%$  and 16% arc nearly equivalent. With the exception of the swept strut, no strut form tested offers a significant advantage over struts 1 or 4. Struts with  $x/c = 65\%$  are of little practical value due to high section drag and other undesirable effects. However, the

relationship between spray drag and the surface area wetted by the spray suggests that drag can be reduced without altering the basic strut form with the addition of a device designed to reduce the wetted surface area. Three types were tested: vertical separation strips, a spray plate, and horizontal spray rails. Only the spray rails were successful in reducing drag.

A brief test was made with a pair of 1/8-inch thick vertical strips located two inches ahead of the trailing edge of strut

Table 2. Mass Flow Rate and Mass Flow Rate Coefficients for Various Strut Configurations

strut Configuration	V ft/sec	T lb	M lb/sec	C <sub>M</sub>
1	24	1.98	3.35	0.349
	20	1.15	2.49	0.312
2A	24	2.03	3.22	0.335
	20	1.09	2.24	0.280
2B	24	2.01	3.20	0.334
	20	1.06	2.16	0.210
3A	24	1.93	3.54	0.369
	20	1.10	2.54	0.318
3B	24	2.30	3.39	0.353
	20	1.34	2.53	0.316
4	24	0.77	1.53	0.283
	20	0.43	1.11	0.247
5A	24	0.82	1.62	0.301
	20	0.47	1.22	0.272
5B	24	0.80	1.29	0.238
	20	0.42	0.87	0.193
6	24	4.61	7.35	0.444
	20	2.86	5.55	0.403
7A	24	4.19	7.02	0.424
	20	2.36	5.08	0.369
7B	24	3.54	6.72	0.407
	20	2.50	4.58	0.333
8A	24	1.68	3.19	0.332
	20	0.93	2.30	0.288
8B	24	2.10	2.30	0.344
	20	1.25	2.44	0.306

configuration 3A. The strips were able to separate the spray sheet from the strut as intended but did not reduce drag. This was probably because additional pressure drag was exerted on the strips and the surface area wetted by the spray was reduced by only slightly more than one-third.

A large flat plate was attached to strut 1 parallel to the flow, which created a spray shield. This did not appear to reduce the total wetted surface area since the spray sheet covered the underside of the plate in a pattern very similar to the flow over the strut in the absence of the plate. No measurable change in drag was observed.

A series of spray rails was added to strut 1. Each rail was a 1/8-inch-thick wood strip faired at both ends. The rails were mounted parallel to the flow with their centerlines 3/4-inches apart. A single rail was sufficient to turn the spray as shown in Figure 15. These rails produced a substantial reduction in spray drag. In Figure 16 the drag at 20, 22, and 24 ft/sec on strut 1, both with and without rails, is plotted against the elevation of

the upper edge of the strut. At 24 ft/sec a maximum reduction of 0.35 lb of drag occurred when the lowest set of rails was about 5% of the chord above the waterline. At an elevation of 20% of the chord, the savings was about 0.25 lbs.

Later, 1/16-inch-thick plastic rails were glued on struts 3 and 8, which were then tested in configurations 3A and 8A. Results arc shown in Figure IX. Ventilation was more severe when these rails were submerged since they were not faired. These rails reduced drag but not as much as those on strut 1. The maximum savings in both cases was about 0.25 lb.

### Conclusions

The results of this investigation of the spray drag produced by fourteen strut configurations are briefly summarized as follows:

1. Spray drag is partially dependent on strut form as well as strut thickness. Struts with blunt leading edges tend to produce more spray drag.

2. Empirical equations were deduced for several strut series in the region  $0.12 \leq t/c \leq 0.2$ . For double arc struts they are

$$D_{\text{spray}} = 0.003 \text{ qct} + 0.06 \text{ qt}^2 \quad \text{when } x/c = 65\%,$$

$$D_{\text{spray}} = 0.011 \text{ qct} + 0.08 \text{ qt}^2 \quad \text{when } x/c = 50\%,$$

and

$$D_{\text{spray}} = 0.009 \text{ qct} + 0.13 \text{ qt}^2 \quad \text{when } x/c = 35\%.$$

The equation for the 66-series airfoil is

$$D_{\text{spray}} = 0.036 \text{ qct} - 0.03 \text{ qt}^2.$$

3. A cusped leading edge decreases spray drag but does not produce an advantage for a fixed waterplane area. Sweeping a double arc strut decreases the spray drag for a given waterplane area by decreasing the surface area wetted by the spray.

4. Skin-friction due to the wetting of the strut surface by the spray sheet is the primary source of spray drag. Therefore spray drag is expected to be Reynolds number dependent.

5. The mass rate of flow in the spray sheet depends on  $t/c$  and the Froude number but not on  $x/c$ . However, blunter bodies send the spray up at higher angles which wets more strut area. Blunt sections are not recommended for semisubmerged ships since the spray may strike the platform.

6. The losses caused by the upward acceleration of the spray contributed only a small fraction of the total spray drag of slender struts at moderate Froude numbers.

7. The momentum in the spray sheet is sufficient to create a large pressure drag on any object it may strike.

8. Horizontal spray rails can produce a substantial reduction in spray drag.

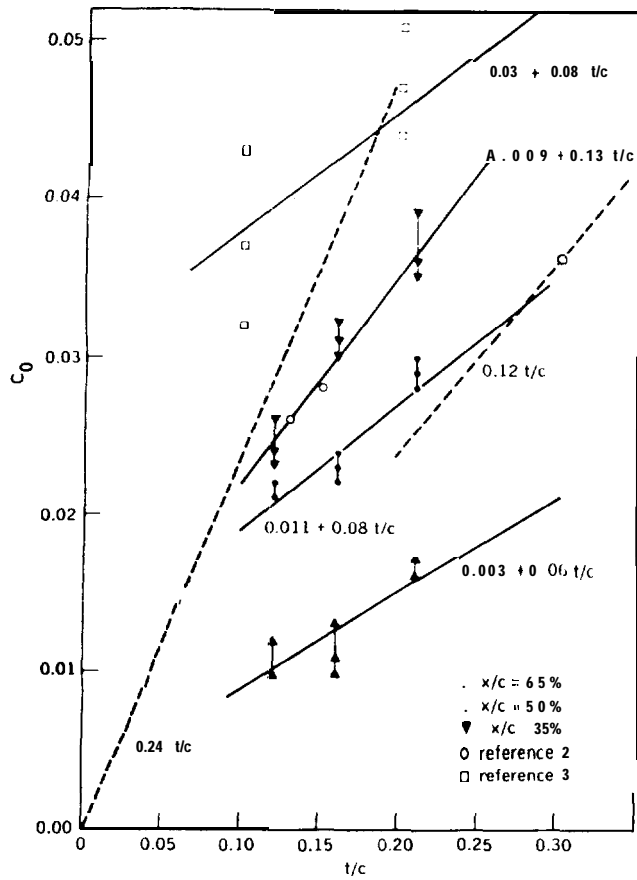


Figure 1. Spray Drag Coefficients for Double Arcs

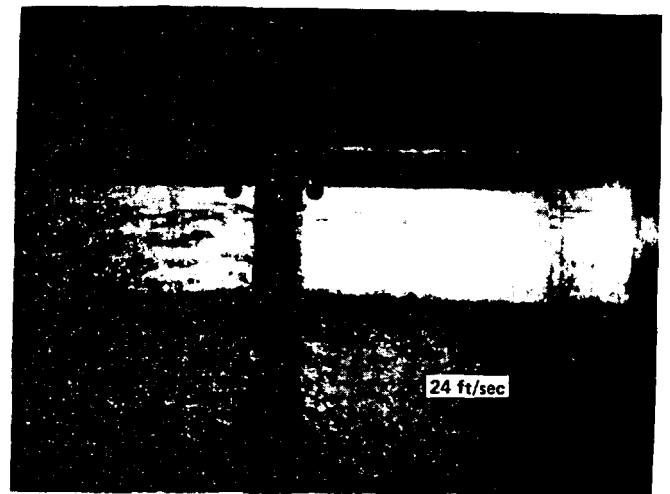
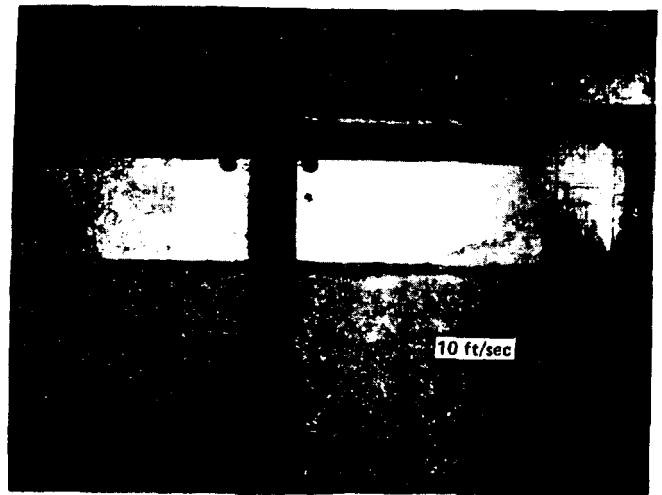


Figure 3. Spray Sheets Produced by Strut 1 at 10 and 24 ft/sec, where  $t/c = 0.16$  and  $x/c = 0.50$

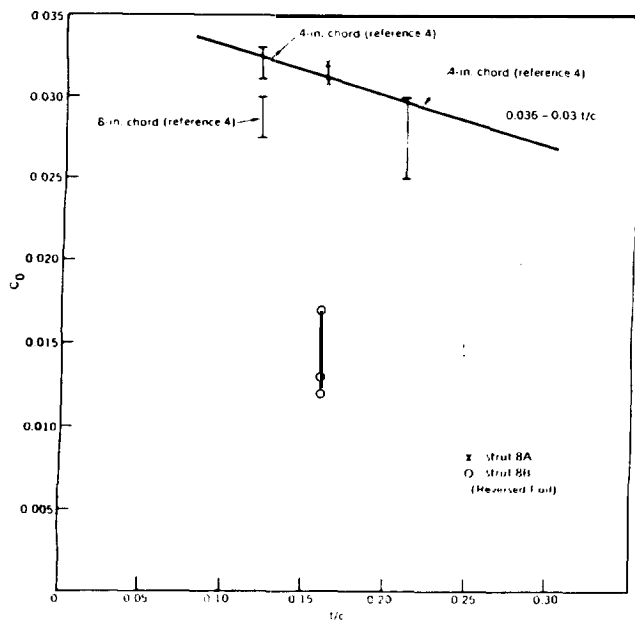


Figure 2. Spray Drag Coefficients for 66-Series Airfoils

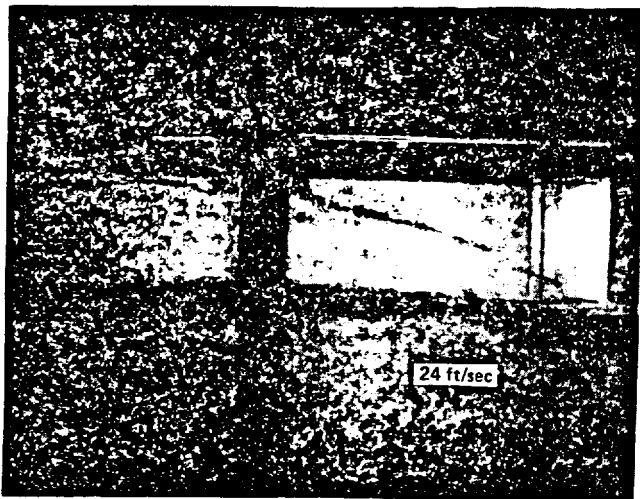
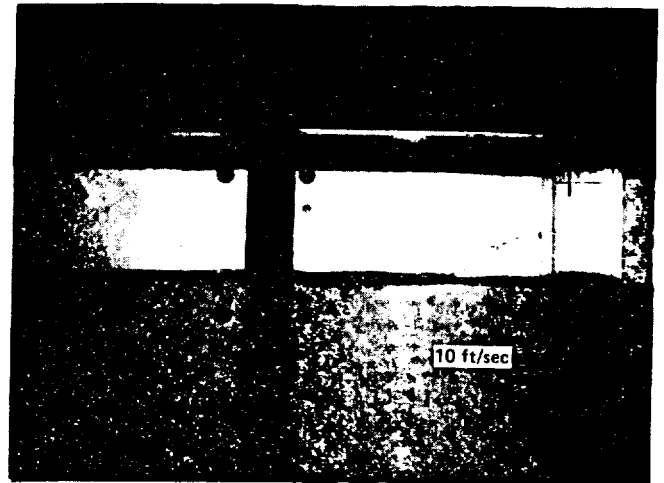
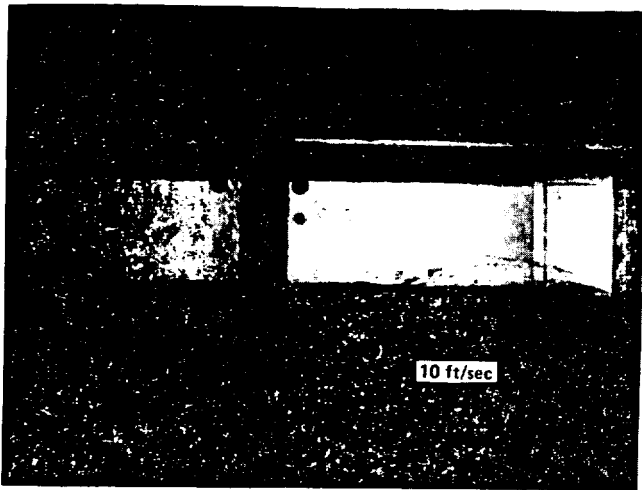


Figure 4. Spray Sheets Produced by Strut 2A at 10 and 24 ft/sec, where  $t/c = 0.16$  and  $x/c = 0.50$  (Cusped)

Figure 5. Spray Sheets Produced by Strut 3A at 10 and 24 ft/sec, where  $t/c = 0.16$  and  $x/c = 0.35$

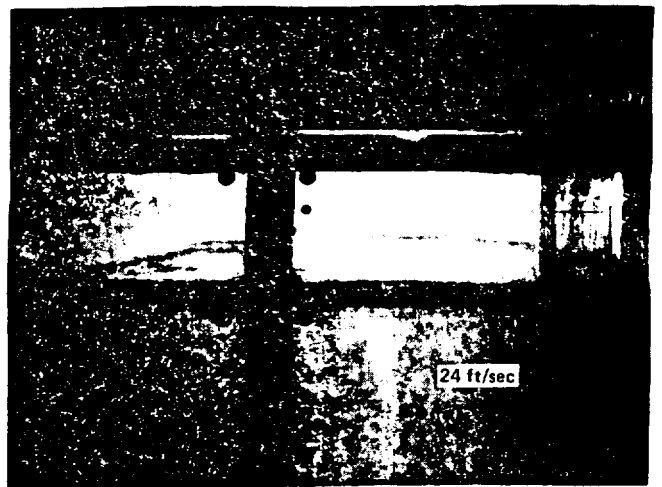
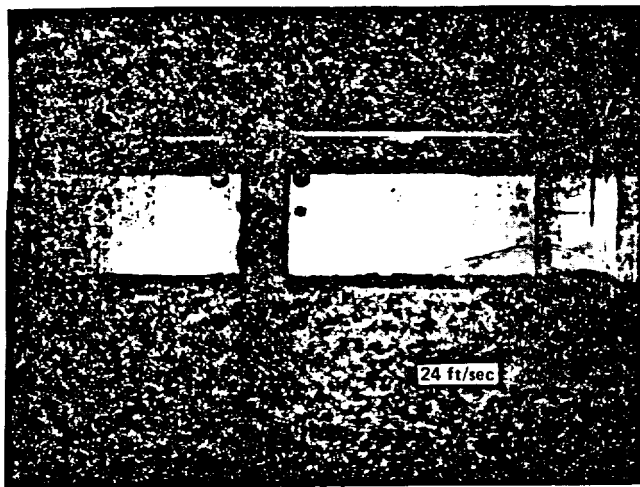
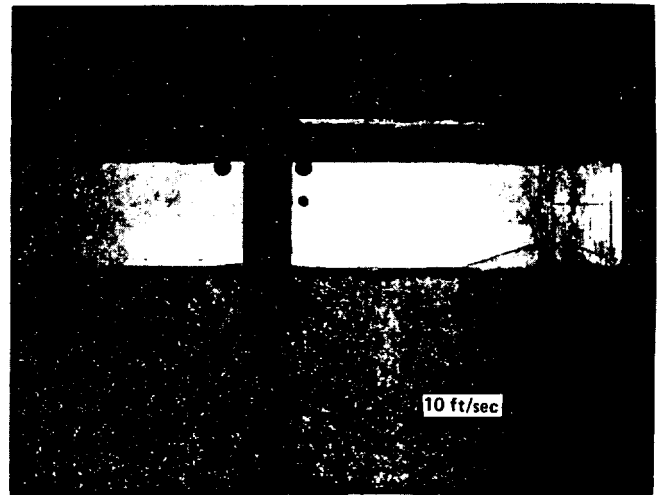
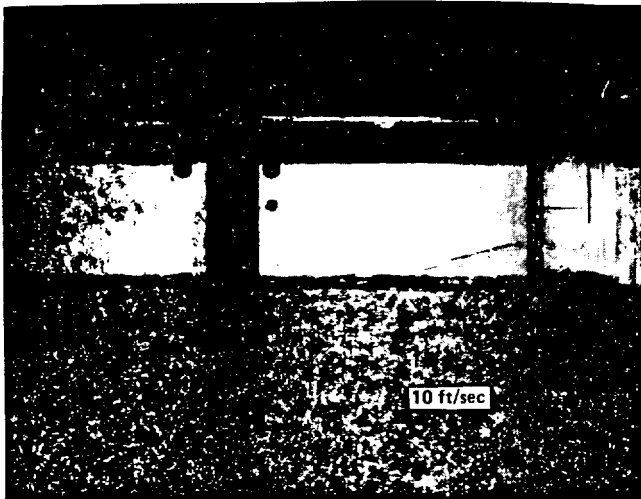


Figure 6. Spray Sheets Produced by Strut 3B at 10 and 24 ft/sec, where  $t/c = 0.16$  and  $x/c = 0.65$

Figure 7. Spray Sheets Produced by Strut 4 at 10 and 24 ft/sec, where  $t/c = 0.12$  and  $x/c = 0.50$

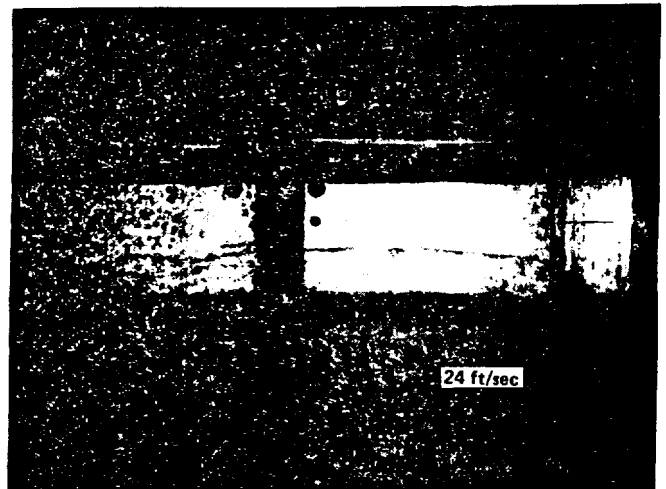
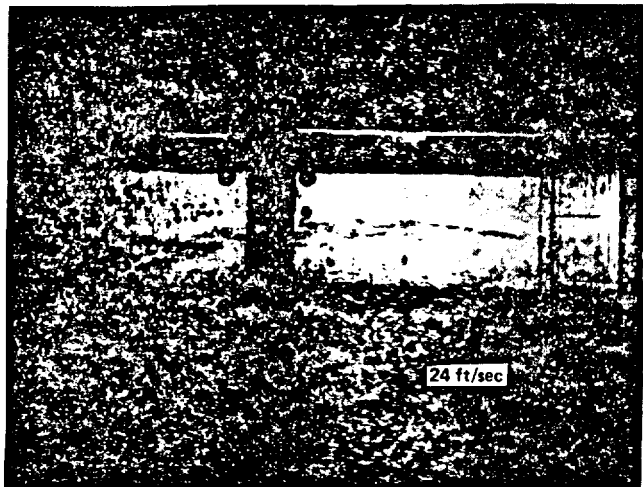
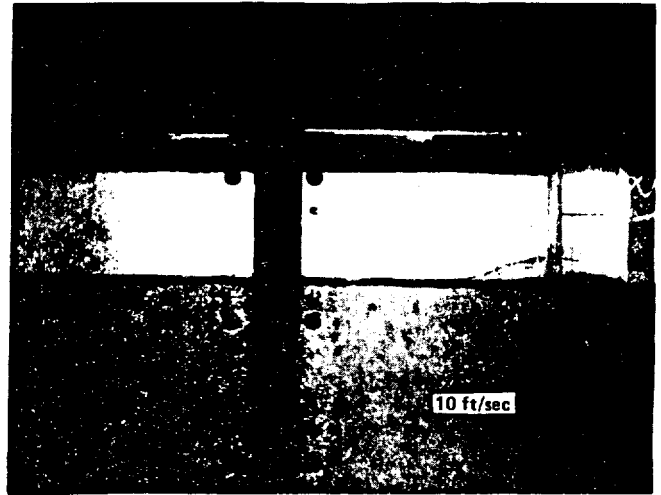
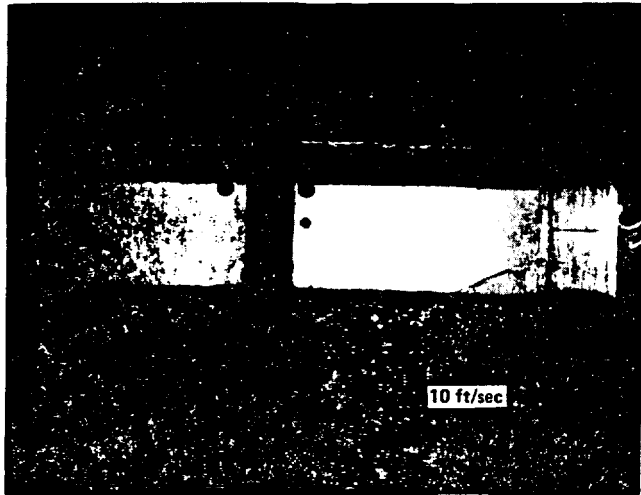


Figure 8. Spray Sheets Produced by Strut 5A at 10 and 24 ft/sec, where  $t/c = 0.12$  and  $x/c = 0.35$

Figure 9. Spray Sheets Produced by Strut 5B at 10 and 24 ft/sec, where  $t/c = 0.12$  and  $x/c = 0.65$

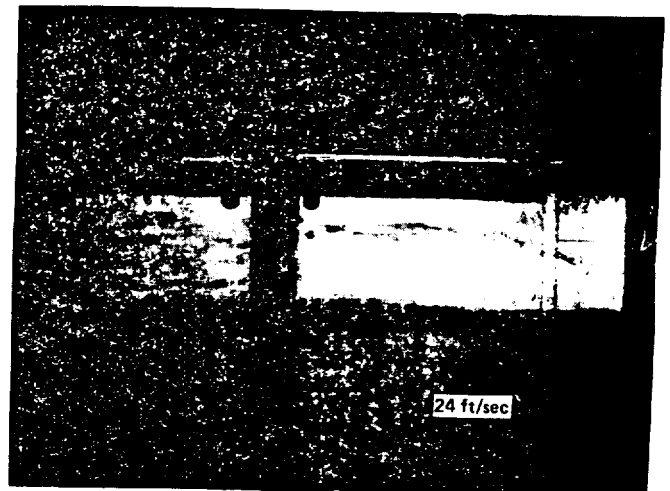
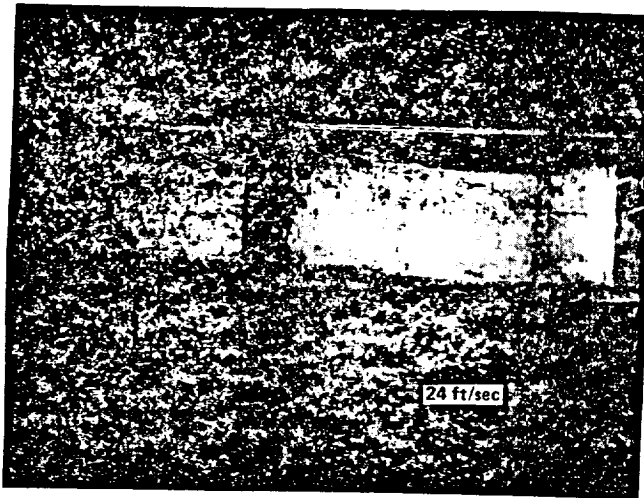
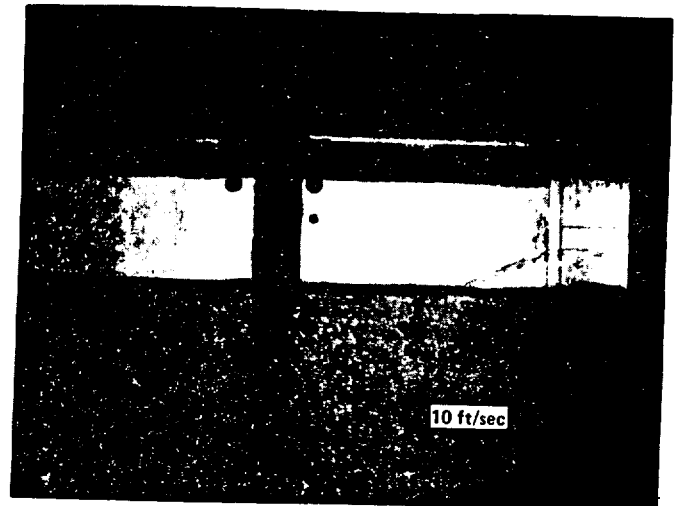
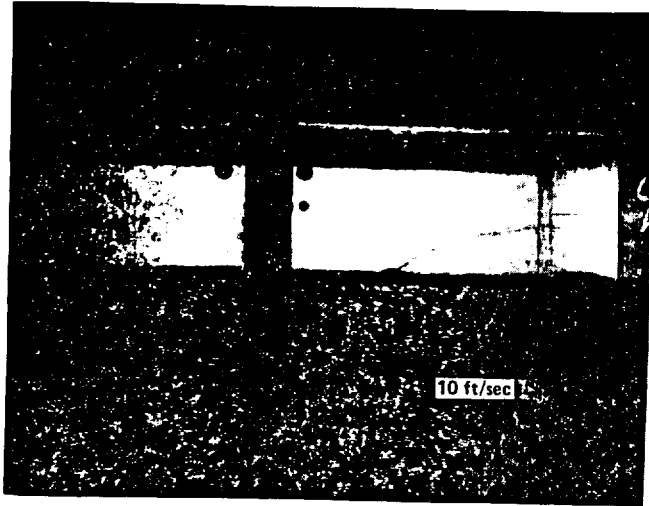


Figure 10. Spray Sheets Produced by Strut 6 at 10 and 24 ft/sec,  
where  $t/c = 0.71$  and  $x/c = 0.50$

Figure 11. Spray Sheets Produced by Strut 8A at 10 and 24 ft/sec,  
where  $t/c = 0.16$  (66-series airfoil)

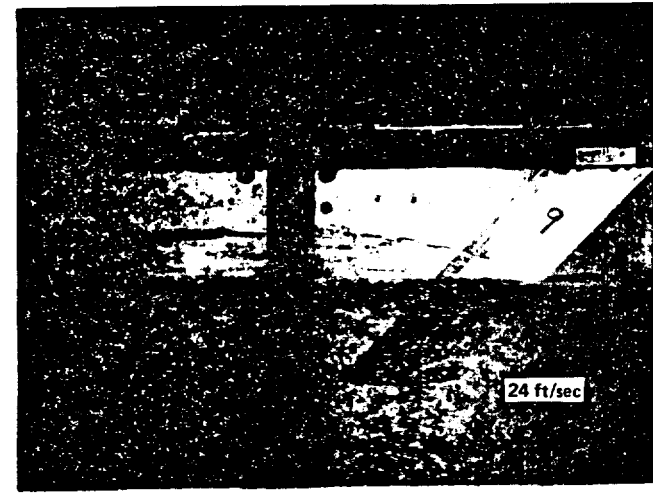
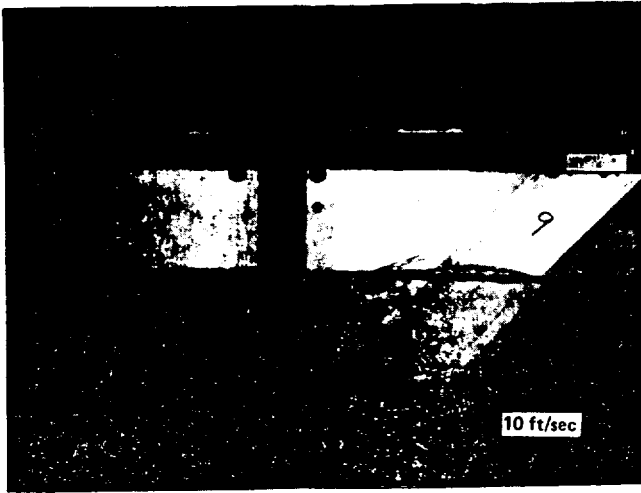


Figure 12. Spray Sheets Produced by Strut 9 at 10 and 24 ft/sec, where  $t/c = 0.16$  and  $x/c = 0.15$

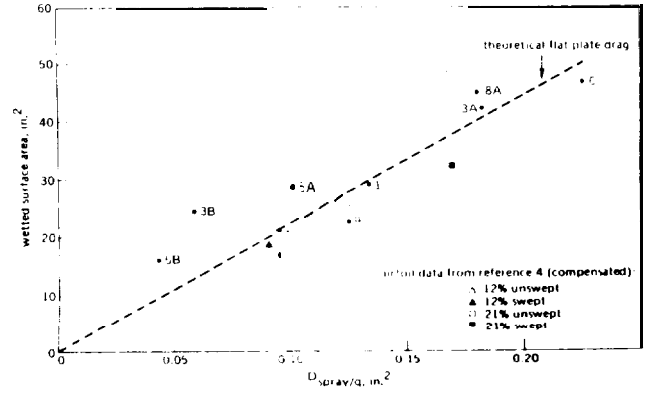


Figure 13. Variation of Spray Drag with Surface Area Wetted by the Spray

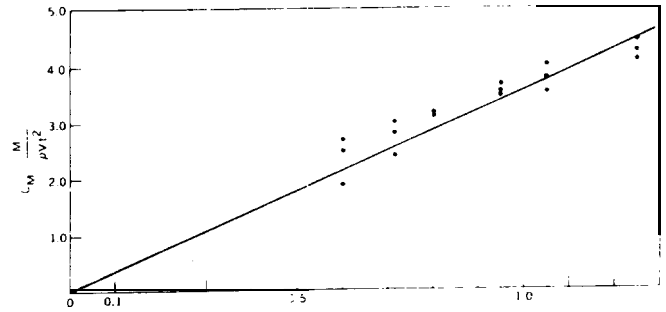


Figure 14. Variation of Mass Flow Rate Coefficient for the Spray Sheet With the Product of the Thickness Ratio and Froude Number

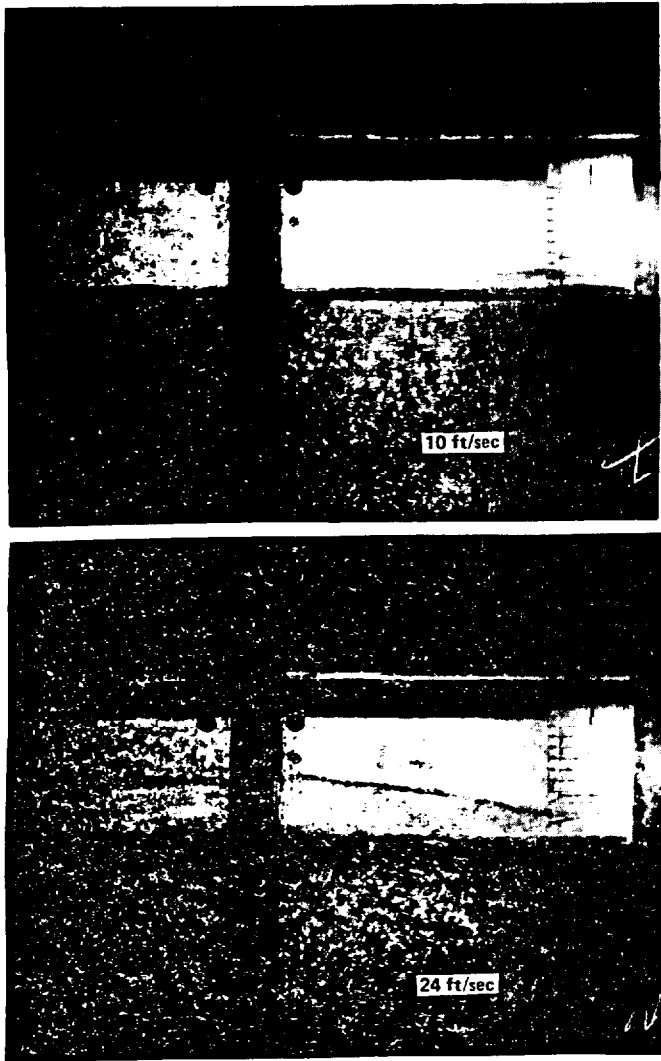


Figure 15. Effect of Spray Rails on Spray Sheets Produced by strut I at 10 and 24 ft/sec

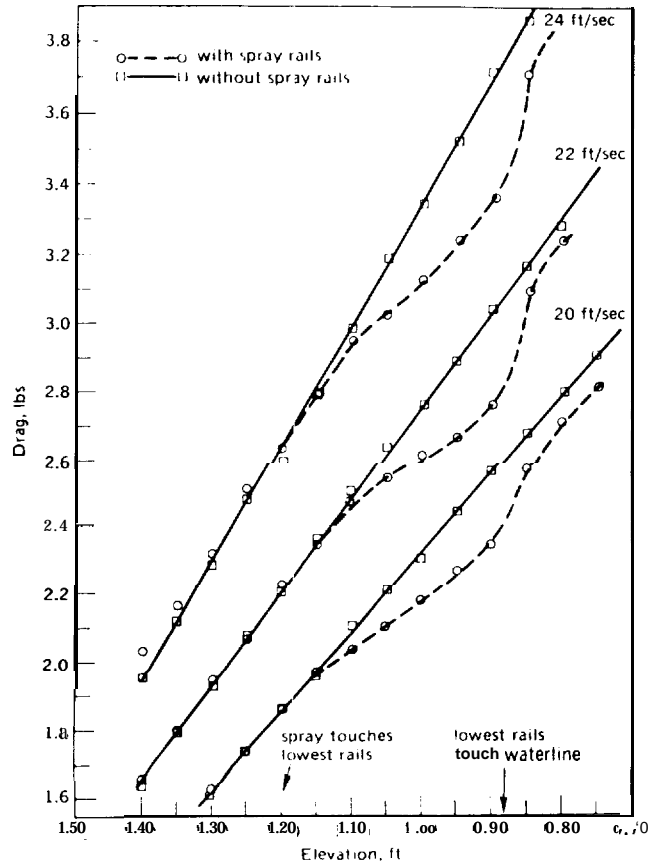


Figure 16. Effect of Spray Rails on Drag of Strut I

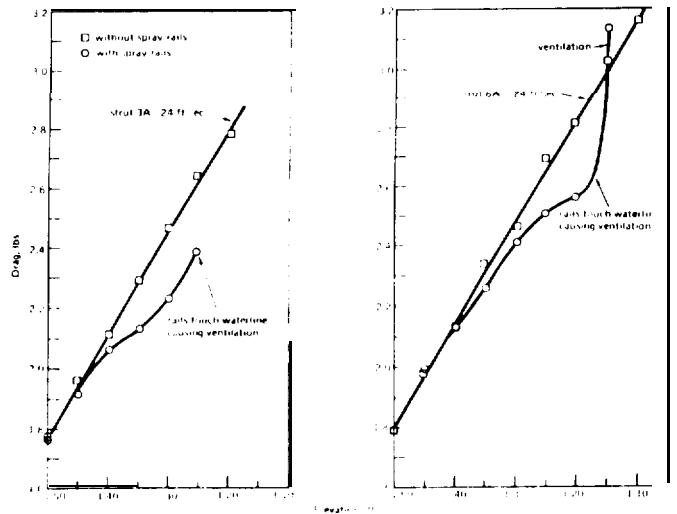


Figure 17. Effect of Spray Rails on Drag of Struts 3A and 8A

Appendix

The experiments described in the main body of this report were conducted under conditions similar to those of previously published experiments. However, struts on an S<sup>3</sup>-type semi-submerged ship operate under somewhat different circumstances. One consideration is the small aspect ratios of these struts (typically from 0.1 to 0.3). Also, maximum Froude numbers correspond to the regime where the spray sheet is just beginning to form.

A second series of spray drag tests were conducted at moderate Froude numbers and small aspect ratios. Two rectangular struts with square tips were tested—strut A1 with a chord of 18 inches and a t/c of 0.15 and strut A2 with a chord of 23.24 inches and a t/c of 0.09. Both struts had a waterplan area of 0.225 ft<sup>2</sup>. They were of the symmetric double arc type with sand strips to trip turbulence. These tests were conducted at drafts of 2.4, and 6 inches at speeds between 7 and 18 fps.

Before spray drag could be evaluated, wave drag had to be accounted for. The theoretical wave resistance for a strut in a canal of finite depth (corresponding to the tow basin) was calculated based on linearized thin ship theory. Due to the small aspect ratios, it was anticipated that spray drag might not be totally independent of draft. Therefore, the section drag was based on the Schoenherr formulation with overvelocity and form drag taken into account.<sup>(2)</sup> The sum of the tip drag and spray drag were then calculated with the formula

$$D_{TIP} + D_{SPRAY} = D_{MEASURED} - D_S - D_{WAVE}$$

where  $D_S$  is the theoretical drag for two-dimensional flow over the strut section and  $D_{WAVE}$  is the theoretical wave drag. The resulting values for  $(D_{TIP} + D_{SPRAY})/q$  are shown in Figures A-1 and A-2. These values are equivalent to a drag coefficient based on an area of 1.0 ft<sup>2</sup>.

If it is postulated that spray drag is essentially zero at 7 fps, then the spray drag coefficient can be identified as the increase in  $(D_{TIP} + D_{SPRAY})/q$  at higher speeds and the tip drag coefficient as the value at low speeds. Empirical results for the tip drag of square tips on rectangular wings indicate that  $D_{TIP}/q$  should be about  $3.8 \times 10^{-3}$  (ft<sup>2</sup>) for strut A1 and  $2.2 \times 10^{-3}$  (ft<sup>2</sup>) for strut A2. Low Froude number results deviate from these values, particularly for the case of strut A1. This probably results from differences between theoretical and experimental values for both tip and section drag. Since these differences do not depend on Froude number, they should have no significance for the spray drag results.

The figures show spray drag coefficients clearly developing with increasing speeds and at 18 fps reaching values equivalent to those predicted by earlier experiments. The maximum speed of S<sup>3</sup>-type semi-submerged ships correspond to about 10 fps for these struts. At 10 fps the spray drag coefficients of struts A1 and A2 have increased to about 30% and 20% of their high-speed values, respectively.

Spray rails similar to those tested in the first series of experiments were also tested at low Froude numbers. The rails had little effect at speeds below 14 fps but showed spray drag savings of 15% and 35% at 18 fps for struts A1 and A2, respectively. On the other hand, tests with S<sup>3</sup> models have demonstrated that spray rails can reduce the total drag on this model by as much as

3% at the maximum speed. Visual observation suggested that this drag reduction was actually due to the rails preventing the spray from striking the bottom of the structure bridging the two hulls. The rails are most effective in keeping this structure dry if they are placed high on the strut on both inboard and outboard sides.

In general, these experiments show that due to low Froude numbers and favorable strut sections, spray drags on S<sup>3</sup>-type semi-submerged ships are much lower than previous empirical estimates<sup>(2,3)</sup> indicate. Also, spray rails appear to be beneficial for these ships primarily since they divert spray from the bridging structure.

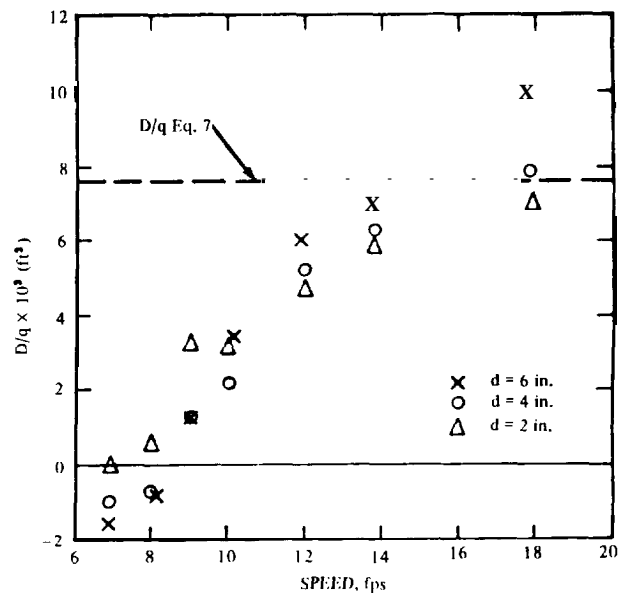


Figure A-1. Total Tip and Spray Drag for Strut A1

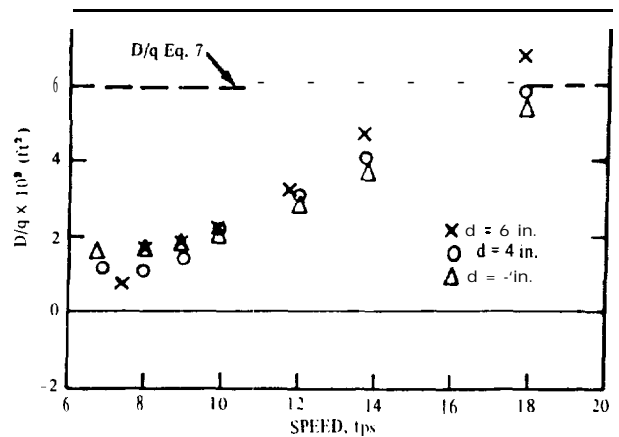


Figure A-2. Total Tip and Spray Drag for Strut A2

### References

1. T. G. Lang. *Naval Feasibility Study of the NUC Semi-Submerged Ship Concept*. "Part I: Introduction, General Characteristics, and Summary" NUC Tech. Pub 735. Naval Undersea Res. & Dev. Ctr. (Sept 1971).
2. S. F. Hoerner. *Fluid-Dynamic Drag* (1965).
3. D. Savitsky and J. P. Breslin. *Experimental Study of Spray Drag of Some Vertical Surface-Piercing Struts*, Davidson Laboratory Report 1192 (Dec. 1966).
4. C. W. Coffee and R. E. McKann. *Hydrodynamic Drag of 12 and 21 Percent Thick Surface-Piercing Struts*. National Advisory Committee for Aeronautics, NACA Tech. Note 3092 (Dec. 1953).
5. I. Kaplan, *Tests of Surface-Piercing Struts*, Stevens Institute of Technology, Stevens ETT Report 488 (April 1953).
6. S. F. Hoerner, *Some Characteristics of Spray and Ventilation*, Gibbs and Cox, Inc.. Tech. Report No. 15 (Sept 1953).